

Quasi-three-dimensional modelling of the morphology of longshore bars

N. Drønen, R. Deigaard *

Department of Mechanical Engineering, Technical University of Denmark, DK-2800 Lyngby, Denmark

Received 20 April 2005; received in revised form 24 August 2006; accepted 29 August 2006
Available online 1 November 2006

Abstract

A morphological quasi-three-dimensional (Q3D) area model for barred coasts has been developed. The model combines a two-dimensional depth integrated model for wave-driven currents with a model for undertow circulation currents. The combined model makes a simultaneous simulation of the bar-forming processes associated with the undertow and the horizontal wave-driven circulation currents, which may cause instabilities of the bar and the formation of rip channels. Situations with normal and oblique wave incidence are considered. Compared to the depth integrated approach the Q3D model produces less pronounced alongshore irregularities for obliquely incident waves. For normal incident waves the Q3D model produces a crescentic bar while the depth integrated model predicts almost straight sections of the bar interrupted by rip channels. The sensitivity to variation of wave angle and beach slope is further investigated.

© 2006 Elsevier B.V. All rights reserved.

Keywords: Coastal morphology; Longshore current; Wave-driven currents; Surf zone; Undertow; Sediment transport; Quasi-three-dimensional model; Barred beach; Rip channels; Crescentic bars

1. Introduction

Prediction of the dynamic behaviour of near-shore bar systems can be of great importance. Sometimes the alongshore variability is low and the assumption of alongshore uniformity may be imposed with success. At other times the three-dimensionality of the system can be considerable and must be taken into account. The bar configuration is of significance for the longshore and the cross-shore sediment transport. The bar geometry is also important for near-shore circulation currents and mixing and dilution of water coming into the coastal area by seepage or discharged by river flow. No reliable method for quantification of the evolution of complex bar morphology has yet been developed, and basic research is still needed.

A number of mechanisms have been proposed as being important for the formation of bars, including non-uniform mass transport velocity stemming from recurrence due to non-linear interaction between the wave and free (released) higher

harmonics (Boczar-Karakiewicz et al., 1987) and Bragg scattering and reflection from the shore (Yu and Mei, 2000). For longshore breaker bars local processes related to vortices generated at the plunge point for plunging breakers have been considered (Miller, 1976), and horizontal diffusion of suspended sediment from the zones of high wave agitation in the surf zone has been analysed by Black et al. (2002). On a dissipative beach under erosive wave conditions the cross-shore transport associated with the undertow is often found important for the bar generation (Dean et al., 1992). Undertow is a vertical circulation current in the surf zone with an offshore directed flow near the bed, which is driven by the vertical distribution of the momentum flux in breaking waves (e.g. Dyhr-Nielsen and Sørensen, 1970; Dally and Dean, 1984; Svendsen, 1984; Deigaard and Fredsøe, 1989). The undertow causes an offshore directed sediment transport in the surf zone. Outside the surf zone the cross-shore transport mechanisms are weaker and may be in the on- or the offshore direction. The sediment thus tends to accumulate around the breaker line forming a breaker bar. Many of the morphological profile models representing this mechanism predict the formation of multiple bars (e.g. Brøker Hedegaard et al., 1991; Roelvink and Brøker, 1993; Rakha et al., 1997). After breaking over one bar the waves

* Corresponding author. Present address: DHI Water and Environment, Agern Allé 5, DK-2970 Hørsholm, Denmark.

E-mail addresses: dronen2@rymarksvaenget.dk (N. Drønen), rd@dhigroup.com (R. Deigaard).

reform inshore of it to break once more further inshore, where the next is then formed. Under irregular waves the transition between the transport due to the undertow and other effects, for example due to wave skewness, which dominate outside the surf zone is gradual, and the changing wave conditions may give onshore directed transport over a bar crest under gentle conditions and offshore directed transport under severe wave conditions where the ratio between the wave height and the water depth is higher, as discussed by Ruessink and Terwindt (2000).

For the present morphological modelling study the undertow has been considered as the cross-shore transport mechanism responsible for generating the bar profile, and it has not been an object to make a comparison between the different possible mechanisms. In this study constant wave conditions are assumed, and each case simulating the formation and development of longshore bars starts from a plane (constant slope) beach profile. The bars are therefore continuing their development under the same incoming wave conditions that formed them from the start, and the situation may be taken to represent the effect of an erosive wave condition without considering the more gentle reforming conditions, which are often important under natural conditions.

Bars have a wide range of behaviour in time and space. Perhaps most evidently, they move in the cross-shore direction. On the time scale of decades, multi-bar systems may be temporally cyclic and a net offshore migration of the individual bars may occur, typically under severe wave conditions with significant wave breaking over the bar (Ruessink and Terwindt, 2000). When sufficiently far offshore the bar may decay completely and new bars form further inshore. On a smaller time scale a bar system can be very dynamic with the bar crests moving on- and offshore, somewhat correlated with the variations in the wave climate (e.g. Plant et al., 1999). On the same time-scale the bar may also break up to form a three-dimensional system, and the short term variability of the distance of the bar crest from the shoreline at a given position may be due to changing alongshore non-uniformities (Ruessink et al., 2000; van Enckevort et al., 2003).

Non-uniformity of a bar is often associated with the formation of rip channels, which are depressions interrupting sections of the bar. In the plan form, the bars can also be crescentic or form oblique patterns. The three-dimensional features are often found to repeat themselves down the coast in an almost regular pattern or as more irregularly distributed patterns. Typical length scales of these features are in the order one to many times the width of the surf zone (100 to 1000 m along-shore) (e.g. van Enckevort and Ruessink, 2003; van Enckevort et al., 2003). Observations have shown how the along-shore undulations tend to lengthen and decrease in horizontal (cross-shore) amplitude for increasing wave power, thus seemingly tending towards an almost linear bar. For more gentle conditions these long straight configurations may again start to produce along-shore variations (Lippman and Holman, 1990).

The three-dimensionality of the longshore bars must be the result of an interaction between morphology, hydrodynamics and sediment transport in the surf zone with a complex interplay

between horizontal wave-generated current patterns and the cross-shore sediment transport which may form and maintain a longshore bar in the coastal profile.

A bar with an along-shore variation in the crest elevation is affecting the wave breaking so that the driving forces also vary in the along-shore direction. When the waves break the shore-normal component of the radiation stress decreases towards the shore. This acts as an onshore directed forcing, which creates an increase in the water level towards the shore, the wave set-up. If the bar crest is higher, more wave energy is spent due to breaking, and the onshore forcing is stronger. For normal wave incidence (wave angle: zero) this induces circulation in the horizontal plane with flow toward the shore at the shallow parts of the bar and away from the shore at the deeper parts of the bar crest, Fig. 1A. The circulation currents will redistribute the sediment, causing changes in the bar morphology, and in some conditions further amplify the non-uniformities originally being the cause of the circulation currents. A closed morphological feedback loop thus exists, which gives the beach what we may call its 'inherent' (or 'free') behaviour where the alongshore wave length is not determined directly from the forcing. A very important factor in this context is the angle of incidence, because it is related to a qualitative 'shift' in the flow picture. For obliquely incident waves, the longshore wave-driven current is of significance through the effect of inertia and contraction of the streamlines. The longshore current flows through the forcing field, and a fluid element experiences an alternating on- and offshore forcing, causing a meandering pattern in the flow, Fig. 1B. In this case the small perturbations may grow as well as migrate in the direction of the longshore current and the littoral drift. It is now a well-established theory that an otherwise straight uniform coast can undergo sudden changes with along-shore variations growing spontaneously due to this mechanism of instability alone (originating from Hino, 1974). The morphological instability has been studied quite intensively within the framework of linear stability analyses for beaches with monotonous profile and for barred beaches (examples being: Christensen et al., 1994; Falques et al., 1996; Deigaard et al., 1999; Caballeria et al., 2002; Calvete et al., 2005). These studies indicate that the morphological instability can occur for practically any realistic profile shape, but it is strongest for a barred profile and at a direction of wave propagation normal to the coastline.

In order to describe the development of the bar morphology with a complex three-dimensional configuration, a more complete non-linear model description is needed, involving a system of numerical models for the wave-, current- and sediment transport fields with a resulting morphological update of the morphology. Examples of such models are described in the review of DeVriend et al. (1993). Examples of the application on the specific problem of irregular longshore bars are given by Reniers et al. (2004) and by Damgaard et al. (2002). The existing model tools have until recently been using a description based on either long-shore uniformity (2D-Vertical (2DV) profile models) or neglecting the cross-shore transport mechanisms (2D-Horizontal (2DH) area model). The outcome of these models have to some degree been successful, particularly the

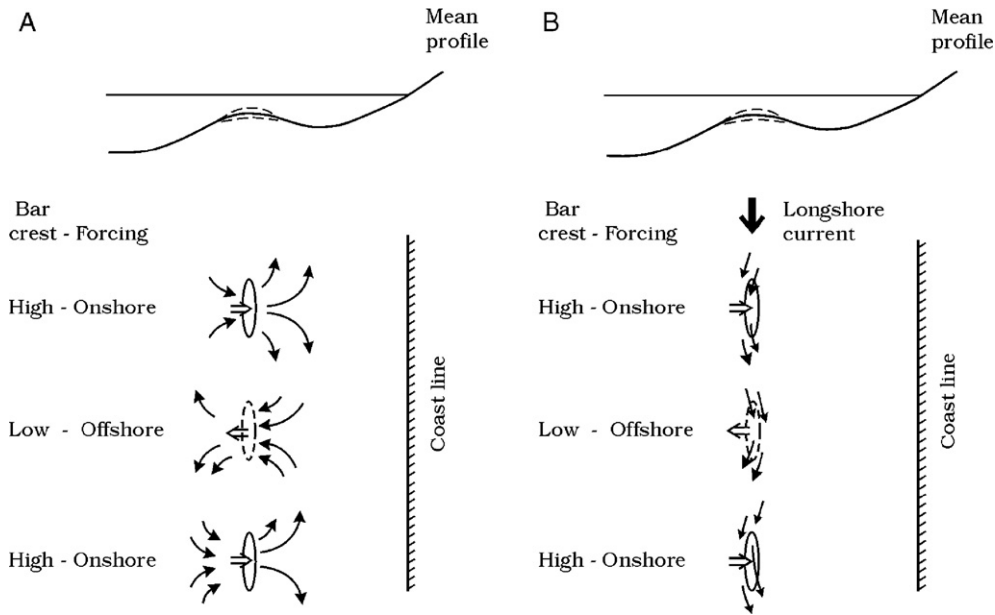


Fig. 1. Wave-driven circulation current over bar with alongshore periodic variations in the bar crest level. A: normal wave incidence with no longshore current. The excess driving force and the circulation current is directed onshore over the elevated parts of the bar crest and offshore over the depressed parts. B: Oblique wave incidence with a longshore current. The excess forcing is directed onshore over the elevated parts of the bar crest and offshore over the depressed parts. In combination with the longshore current the forcing generates a meandering flow along the bar crest.

2DH area models. Morphological models that incorporate the combined effect of bar generation and topographically induced circulation currents is a relatively new field and only a few model studies have been made.

A potentially important question, which has not yet been answered is how the morphological development of the bar is affected by the interaction of the bar generating mechanisms (notably the cross-shore sediment transport due to the undertow) and the horizontal circulation currents generated by the wave breaking on a non-uniform coastal profile. This interaction can be important for the bar configuration in the horizontal plane, but also for the bar profile development because if the bar is not uniform, the main assumption behind most coastal profile models will be violated.

The present work has addressed this question by a direct and simple implementation of a combination of cross-shore vertical circulation (undertow) and horizontal circulation currents in a morphological model. This will enable a description of the bar as it grows and migrates in the cross-shore direction and as it may generate along-shore variability due to a morphological instability mechanism. The model system developed for this study has been made as simple as possible while still maintaining a realistic representation of the relevant processes. The principle applied is a so-called quasi-3-dimensional or Q3D model (DeVriend and Stive, 1987) where a depth integrated two-dimensional flow model is combined with a model for the velocity profiles including secondary flow normal to the mean depth integrated flow direction. The undertow is represented by the secondary flow, and even in the case of a uniform longshore current the undertow will be represented (cf. Svendsen and Lorenz, 1989) and make the direction of the sediment transport deviate from the depth integrated streamline and cause the

formation of a longshore bar. The present study is a continuation of the work by Drønen and Deigaard (2000). It is an extension of the work by Damgaard et al. (2002), which uses a 2DH model without any mechanisms forming the bar, and the work of Reniers et al. (2004), which considers an embayed beach without longshore current and simulated the evolution of a bar prescribed in the initial bathymetry. Reniers et al. (2004) includes bar-forming mechanisms in the form of an undertow, wave asymmetry and interaction of short- and long period waves, further the study investigated the significance of directional spreading of the normally incident waves.

2. The model system

2.1. Morphological model

The present model system is composed by four elements: a wave model, a Q3D hydrodynamic model, a sediment transport model and a procedure to describe the bed evolution. The morphological development in time and space is found by a numerical time-integration of the mass balance of sediment:

$$\frac{\partial h}{\partial t} = \frac{1}{1-n} \nabla \cdot \vec{q}_s = \frac{1}{1-n} \left(\frac{\partial q_{sx}}{\partial x} + \frac{\partial q_{sy}}{\partial y} \right) \quad (1)$$

with h being the still water depth, \vec{q}_s the sediment transport field — as determined by the model, q_{sx} in the x -direction and q_{sy} in the y -direction — and n the porosity of the bed.

The morphological equation is very simple, but when coupled with a complex model for the sediment transport the numerical integration is not straightforward. A process-based morphological model like the present is a multi-scale problem

with a fast time scale corresponding to the hydrodynamics and a slow time scale associated with the morphological evolution. Within the theory of ordinary differential equations, this type of system will be often be found to be ‘stiff’ in the sense that the flow model reacts immediately to a morphological development, giving also an immediate response in the sediment transport field. It is termed a singular perturbation problem, where a small quantity is present in parts of the entire system. When handling the problem numerically this can result in difficulties, for example in the form of instabilities or drift of the solutions (Hairer and Wanner, 1996).

Possible solutions is to integrate the entire system on the hydrodynamic time scale, which ensures stability, or to apply implicit methods, which albeit have not yet been developed for morphological simulation models. In the present model we have adopted a quasi-equilibrium approach, where the hydrodynamics at each morphological time step are ensured to be stationary (this puts the small quantity to zero and treats the system not as a multi-scale system, but as a so-called set of differential algebraic equations, DAE). The time integration is performed by adopting a second-order Adams predictor–corrector scheme.

2.2. Hydrodynamics

The hydrodynamic model consists of three parts: a model for the wave field, a 2DH model for the depth integrated wave-driven flow, and a Q3D model to represent the deviation of the velocity distribution from the depth integrated flow field.

2.2.1. Wave model

The wave field is modelled by use of the Near-shore Spectral Wind Wave model MIKE21, NSW of DHI Water & Environment. The model represents the wave propagation, refraction and shoaling as developed in the HISWA model as described by Holthuijsen et al. (1989). The model is based on linear wave theory describing the transformation of schematised wave spectra by conserving the first two moments of the wave action spectrum. In each point of the rectangular calculation grid the wave energy is distributed on a number of directional bins to resolve the directional spreading. The wave breaking is simulated by the energy dissipation model of Battjes and Janssen (1978).

The wave conditions (height, period and direction) are specified on the offshore boundary. The model then provides the wave parameters, including the rate of energy dissipation in all points of the rectangular calculation domain.

2.2.2. 2DH hydrodynamic model

The 2DH flow model solves the depth integrated equations for conservation of mass and momentum to describe the wave-driven currents. The model is based on the two-dimensional flow model DUNE, which has originally been developed to describe the two-dimensional flow field in the vertical plane (2DV) over bed forms, Tjerry (1995) and Tjerry and Fredsøe (2005). The model has been extended to include the effect of depth variations over a horizontal area.

The horizontal depth- and time-averaged wave-driven current is represented by the flow components U_i . The subscript i refers to the two horizontal coordinates.

The flow equations read:

$$\begin{aligned} \frac{\partial DU_i}{\partial t} + \frac{\partial (DU_i)U_j}{\partial x_j} + \frac{\partial T_{ij}}{\partial x_j} + \frac{\tau_{b,i}}{\rho} + gD \frac{\partial \bar{\eta}}{\partial x_i} + \frac{F_i}{\rho} &= 0 \\ \frac{\partial \bar{\eta}}{\partial t} + \frac{\partial (DU_i)}{\partial x_i} &= 0 \end{aligned} \quad (2)$$

Where D is the flow depth, t is time, $\tau_{b,i}$ is the bed shear stress, ρ is the density of water, g is the acceleration of gravity, $\bar{\eta}$ is the wave period-averaged free surface elevation and F_i is the forcing of the current.

The horizontal momentum exchange due to the combined action of turbulence and the mean current is written as the lateral shear stresses T_{ij} , which are described through a simple momentum exchange coefficient E :

$$T_{ij} = -ED \left(\frac{\partial U_j}{\partial x_i} + \frac{\partial U_i}{\partial x_j} \right) \quad (3)$$

The value $E=0.2 \text{ m}^2/\text{s}$ was used in the present Q3D simulations.

The bed shear stress $\tau_{b,i}$ is determined by a quadratic friction law corresponding to a hydraulically rough flow condition. The bed roughness is taken as a Nikuradse roughness of $k_N=0.25 \text{ m}$. This roughness, which is larger than the expected surface roughness of a sand bed, has been chosen as a simple way of representing the increased flow resistance due to the combined effect of the turbulence generated in the wave boundary layer and in the mean current (cf. e.g. Fredsøe, 1984).

Further the large flow resistance suppresses the hydrodynamic instability, which leads to the formation of shear waves in the longshore current and would make it difficult to reach a steady-state solution for the flow.

In the present simulations the only forcing F_i is due to the gradient in radiation stresses S_{ij} of the surface water waves:

$$F_i = -\frac{\partial S_{ij}}{\partial x_j} \quad (4)$$

Dingemans et al. (1987) showed that the radiation stress field could be divided into two parts, one which is irrotational and always can be balanced by a change in the mean water surface level, and another which is related to the dissipation of wave energy in the surf zone and may drive a current. Only the part, which may drive a current is included in the model, giving:

$$F_i = \frac{\text{DISS}_r}{c} e_{i,ws} \quad (5)$$

Where DISS_r is the wave energy dissipation due to the surface rollers (cf. the wave model) in the surf zone. In the model of Battjes and Janssen (1978) the energy dissipation is calculated by considering the breaking/broken waves as being

similar to a bore, and the energy loss is found from the head loss in a hydraulic jump with the same height. The model combines the energy dissipation of the single wave with the assumption that the wave heights are following a Rayleigh distribution. The parameter c is the wave celerity and $e_{i,w}$ or \vec{e}_w is a unit vector in the direction of wave propagation.

The dissipation rate DISS_r is close to the actual rate of energy loss in the wave motion; but following the analysis of Dally and Brown (1995) the gradual change in the kinetic energy of the surface roller is taken into account by introducing a lag between the loss of wave energy and the dissipation DISS_r . In the present model, the wave energy loss DISS_w is found from the simulation in the wave model with the dissipation model of Battjes and Janssen (1978), and the driving force is then found from:

$$\nabla \left(\lambda_r \frac{\text{DISS}_r}{c} \vec{e}_w \right) = \frac{\text{DISS}_w}{c} - \frac{\text{DISS}_r}{c} \quad (6)$$

which gives a lag, λ_r of DISS_r relative to DISS_w in the direction of wave propagation. The lag distance λ_r is scaled by the local water depth: $\lambda_r \approx 5D - 10D$.

The boundary conditions for the 2DH hydrodynamic model are as follows:

- Coastline and offshore boundary: no flow across the boundary and no cross-shore gradient in the alongshore flux.
- Lateral boundaries: periodic condition along the coast is obtained by linking a given outflow boundary with the corresponding inflow conditions. This is applied for both values and the gradients normal to the boundary.

2.2.3. Q3D extension

The three-dimensional mean flow effects are taken into account by a simple quasi-three-dimensional model. The Q3D approach implies that the current velocity profile over the vertical at a given location is determined by the local forcing and the depth integrated flow. The model is chosen as simple as possible while still retaining the relevant mechanisms.

The shear stress distribution is in accordance with the derivations of Deigaard and Fredsøe (1989) and Deigaard (1993). The mean shear stress is linearly distributed over the vertical, and the surface shear stress is taken as the driving force derived through application of Eqs. (5) and (6):

$$\begin{aligned} \vec{\tau} &= \vec{\tau}_b(1-z/D) + \vec{\tau}_s z/D \\ \vec{\tau}_s &= \frac{\text{DISS}_r}{c} \vec{e}_w \end{aligned} \quad (7)$$

where z is a vertical coordinate with origin at the bed and $\vec{\tau}_b$ is the bed shear stress. The velocity profile is found according to the model of Okayasu et al. (1988) where the mean eddy viscosity ν_t is taken to be varying linearly with the distance from the bed. The eddy viscosity is determined by the bed shear stress:

$$\nu_t = z\kappa U_f \quad (8)$$

where κ is von Karman's constant (0.4) and U_f is the friction velocity equal to $\sqrt{\tau_b/\rho}$. Eqs. (7) and (8) result in a log-linear current velocity profile:

$$u_i = \vec{u} = \frac{1}{\rho\kappa U_f} \left(\vec{\tau}_b \ln(z/(k_N/30)) + (\vec{\tau}_s - \vec{\tau}_b)(z - k_N/30)/D \right) \quad (9)$$

The bed shear stress is determined to obtain the right discharge of the velocity profile given by Eq. (9). An Eulerian mean velocity up to the wave trough level will include a mean flow compensating the wave drift. The discharge of the mean velocity profile is therefore to be equal to the flow obtained in the depth integrated 2DH model plus the compensation for the mass drift of the wave motion, the Stokes' drift q_w , and the amount of water carried in the volume of the surface rollers q_r (cf. Svendsen, 1984):

$$\int_0^D u_i dz = DU_i - q_{w,i} - q_{r,i} \quad (10)$$

The wave-related fluxes, both in the direction of wave propagation, are given as:

$$\begin{aligned} q_w &= \int_D^{D+\eta} u_w dz = BcD \left(\frac{H}{D} \right)^2 \\ q_r &= \frac{\text{DISS}_r}{\rho g \beta_r} \end{aligned} \quad (11)$$

Where the relation between the roller volume and the energy dissipation in bores and broken waves (Deigaard, 1989; Dally and Brown, 1995) has been used. For regular broken waves with the period T , the roller volume per unit length of wave front is found as:

$$A = \frac{\text{DISS}_r T}{\rho g \beta_r} \quad (12)$$

The parameter β_r is the slope of the lower boundary of the roller, which has been assumed to be 10° :

$$\beta_r \approx \tan(10^\circ) \quad (13)$$

Linear shallow water wave theory has been applied for calculating q_w . For sinusoidal waves the coefficient B has the value 1/8, for a saw-tooth profile, which is often applied to describe broken waves B is 1/12. In the present model a weighted average has been applied, based on the percentage of broken waves predicted by the model of Battjes and Janssen (1978).

An example of the velocity profiles obtained by the model is given in Fig. 2. It shows the special case of alongshore uniformity, where the alongshore wave forcing is balanced by the longshore component of the bed shear stress resulting in a logarithmic velocity profile of the longshore current. No roller lag has been assumed, the water depth D is 1.33 m and H_{rms} is $0.75D$. The mean velocity is made dimensionless by division

with U_{fs} defined as $\sqrt{\tau_s/\rho}$. Velocity profiles are shown for two wave angles: 10° and 20° .

3. Sediment transport 2DH and Q3D

The sediment transport module of MIKE21 of DHI Water and Environment has been used to calculate the sediment transport. The sediment transport is determined as a function of the wave height and period, the depth integrated current velocity, the water depth and the energy dissipation due to wave breaking. The sediment transport calculation is based on a detailed model for the unsteady boundary layer in combined waves and current (Fredseø, 1984) including the non-linear turbulent interaction between the unsteady near-bed oscillatory boundary layer and the mean current boundary layer. The boundary layer model gives as results the time-varying bed shear stress (magnitude and direction), the instantaneous velocity profiles and the instantaneous distribution of the turbulent exchange factor over the vertical. The sediment transport is split into bed load and suspended load. The instantaneous bed load transport is calculated from the instantaneous bed shear stress using the model of Engelund and Fredseø (1976) and then time-averaged to give the mean transport. The instantaneous sediment concentration profile is found by application of the vertical diffusion equation for suspended sediment (cf. Fredseø et al., 1985). The bed boundary condition is based on the near-bed concentration model of Engelund and Fredseø (1976). For breaking waves a contribution to the turbulent exchange factor due to the near-surface energy dissipation from the breaking is included in the vertical diffusion equation (Deigaard et al., 1986). The instantaneous suspended sediment transport is found as the vertical integral of the product of the velocity and the concentration profiles. The mean transport is found by time-averaging. In MIKE21NSW the wave breaking is represented by the model of Battjes and Janssen (1978), which predicts the ratio of the breaking wave at a given location, and the total transport is found as a weighted average of the prediction for non-breaking and for breaking waves. The use of numerical models — including MIKE21 — for morphological simulations of coastal areas has been described by Nicholson et al. (1997).

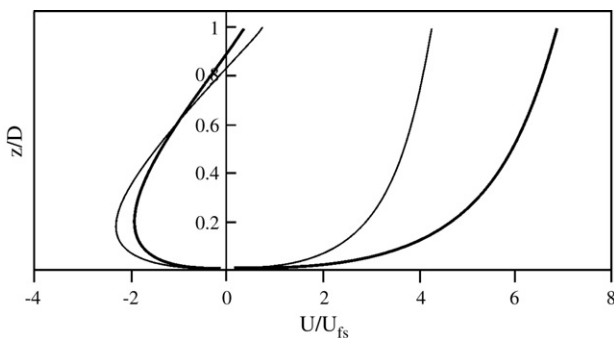


Fig. 2. Longshore (positive) and cross-shore (negative) velocity profiles for alongshore uniform conditions. No roller lag, water depth D : 1.33 m, H_{rms} : $0.75D$. Mean velocity made dimensionless by $U_{fs}(\sqrt{\tau_s/\rho})$. Thin lines, wave angle: 10° , thick lines, wave angle: 20° .

The version of the sediment transport model used in this study assumes the mean current above the wave boundary layer to have a logarithmic distribution. In the Q3D simulations the sediment transport, \vec{q}_{st} , is found for a mean flow velocity corresponding to the direction and magnitude of the mean bed shear stress, $\vec{\tau}_b$, which determines the velocity profile near the bed, where most of the transport is concentrated.

For the purpose of modelling the development of barred profiles the sediment transport \vec{q}_{st} is decomposed into two contributions, namely the transport related to the depth integrated mean current velocity $\vec{q}_{st,c}$ and a transport contribution $\vec{q}_{st,Q}$ related to the Q3D effects. Like the total transport \vec{q}_{st} the current related transport $\vec{q}_{st,c}$ is found from the sediment transport model using the velocity from the 2DH flow model. The Q3D contribution is then found from the vector decomposition of \vec{q}_{st} :

$$\vec{q}_{st} = \vec{q}_{st,c} + \vec{q}_{st,Q} \quad (14)$$

This equation is a key element in Q3D morphodynamic modeling. It illustrates that the integrated morphological phenomenon — the development of a barred beach — is the result of two mechanisms: the 2DH and the Q3D mechanisms. The model results depend on the representation of these two individually as well as the interaction between them.

4. 2DH modelling and simulations of bar instability

The linear stability of a straight, uniform longshore bar under oblique wave incidence was investigated by Deigaard et al. (1999). The analysis was made by use of the depth integrated area model system MIKE21 of DHI Water & Environment. The growth and migration rates were calculated for a perturbation varying harmonically along the coast, and the shape and alongshore wave length of the fastest growing perturbation were determined. Even though the modelling system is fully non-linear the analysis was made for perturbations so small that the deviations from the uniform longshore current and sediment transport could be taken to be linearly dependent on the amplitude of the bed perturbation. This implies that the migration rate is independent of the amplitude and that the growth is varying exponentially in time.

Simulations of the same character have been made with the present model complex, neglecting the Q3D effects i.e. with sediment transport vectors being parallel with the depth integrated flow vectors. The difference from the stability analysis is that the morphological development is simulated, and that the simulation is continued as the perturbation grows and the assumption of linearity is no longer fulfilled.

The barred profile is the same as used in the original linear stability analysis, Fig. 3, with a depth over the bar crest, D_c , of 1 m, depth on the trough, D_t , of 3 m and the bar crest at a distance of 90 m from the shoreline. The bed slope offshore of the bar is 1:43.

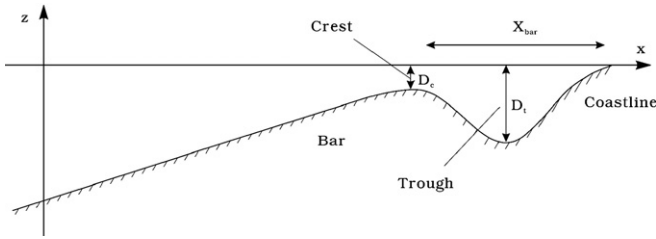


Fig. 3. The initial profile for the 2DH simulations.

4.1. Seeding of the bathymetry

To set off the instability mechanism the initial bathymetry is seeded by adding a series of perturbations varying harmonically in the longshore direction. The maximum wave length was taken to be equal to the length of the simulation domain, and the following were then reduced by a factor 1/2, 1/3, 1/4 — etc. The truncation (longest and shortest) of the wave lengths of the seeding is chosen so that the preferred wave length (of the fastest growing perturbation) is well within the interval. The amplitude was the same for all harmonic components, and each was given a random phase corresponding to a spectrum for white noise. The transverse shape of the seeding was arbitrarily chosen as a ‘bell shaped’ function centred at the bar crest so that the seeding causes harmonically varying depressions and elevations along the bar crest.

The magnitude of the seeding was very small compared to the water depth. Typically the variation in the crest level associated with the seeding was of the order 1 mm. The very small amplitude of the seeding is used to ensure that the initial perturbations in hydrodynamics and sediment transport relative to a uniform condition are linear, and the different components will grow or decay with time similarly to the development in a linear stability analysis. This means that each harmonic of the perturbation can be considered independent of the others. With time the perturbations have grown sufficiently for non-linear effects to be significant, and the morphological evolution becomes non-linear with the alongshore variation being described by more than a single harmonic function. If a simulation had been started with a different seeding (in terms of the spectrum, the phases or the cross-shore shape) the eventual non-linear development will be a different realisation and the details, for example the location of rips will vary, but the main characteristic in terms of the number and the shape of the rip channels are expected to be similar. If the seeding is not of small amplitude the simulation will describe the development of a specific example of a bathymetry under the forcing in the model. A case which resembles this situation is presented later (cf. Fig. 17) where the morphology first evolves under normal wave incidence, after which the wave angle is changed.

No attempt has been made to make the cross-shore variation of the seeding similar to the fastest growing perturbation with the same wave length. This is because the initial exponential growth of the most unstable mode rapidly will obliterate the shape of the original seeding.

5. Morphologic evolution predicted by the 2DH model

The barred profile and the parameter setting are similar to the basic configuration investigated by Deigaard et al. (1999), and the simulations have been used to verify the present model predictions for very small perturbations against the results from that study:

Bed roughness: $k_w=0.25$ m. Horizontal momentum exchange coefficient: $E=0.01$ m²/s; this value is very small and has been chosen to be consistent with the study of Deigaard et al. (1999). Significant wave height: $H_s=1.0$ m ($H_{rms}=0.7$ m). Peak wave period: $T_p=7.5$ s. Deep water wave angle: $\theta=20^\circ$. Grain size of bed sediment: $d_{50}=0.15$ mm. Settling velocity of sediment: $w_s=0.013$ m/s. The computational domain has a length of 3200 m and a width of 600 m. The magnitude of the perturbation or the amplitude of the along-shore topographic variation may be indicated by the quantity σ_{tot} defined as the integrated alongshore variance in the bed level:

$$\sigma(x) = \sqrt{\frac{1}{L} \int_0^L (h(x,y) - \bar{h}(x))^2 dy}$$

and

$$\sigma_{tot} = \int_0^\infty \sigma(x) dx$$

where L is the length of the computational domain and the quantity $\bar{h}(x)$ is the alongshore mean of the bed elevation h at a given distance x from the shoreline. The integrated alongshore variance, σ_{tot} is a measure of the deviation of the bathymetry from the along-shore averaged profile, it is given in m² pertaining to the vertical cross-sectional area normal to the shoreline. The temporal variation in σ_{tot} is illustrated in Fig. 4. During the first 2–3 days the magnitude of the perturbations grows exponentially, and in the later phases the growth slows down.

The temporal evolution of the bathymetry is illustrated in Fig. 5. The simulation was run for a period of 17 days. The simulation was stopped because the bathymetry would become so complex that the number of grid points was insufficient to

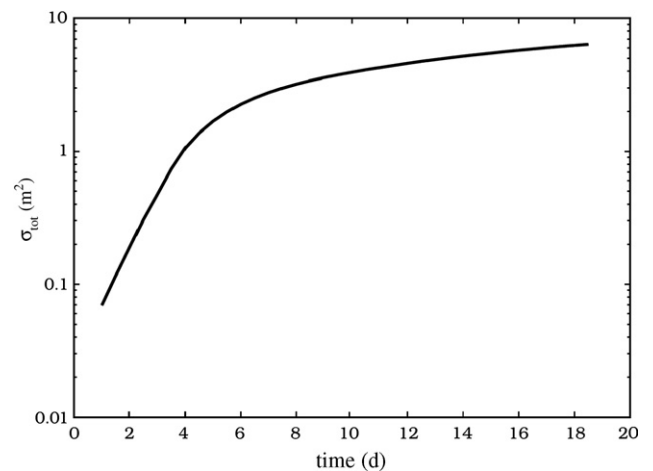


Fig. 4. The temporal variation in the total alongshore variance, σ_{tot} .

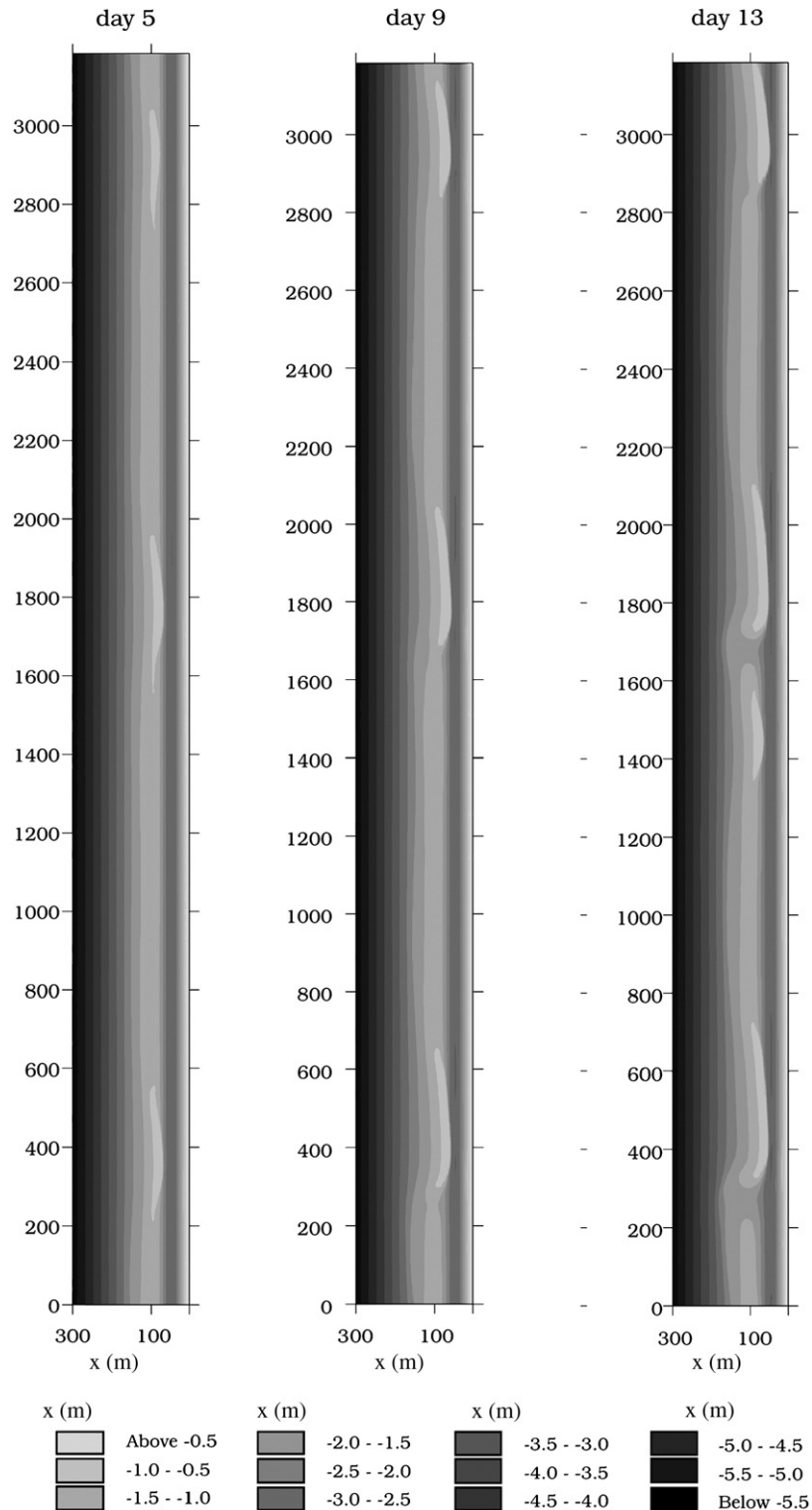


Fig. 5. The temporal evolution of the bathymetry during a 2DH simulation, wave angle: 20° .

give a reliable resolution. If the simulation continued the bed slope would locally be very large and the hydrodynamic model is expected to blow up. The model does therefore not develop a dynamic equilibrium condition with statistically constant properties of the rip channels. The final bathymetry is shown in Fig. 6 together with the flow field and the distribution of the

energy dissipation in the wave model. The latter may be taken as a proxy for the pattern of the surf zone observed via the ARGUS video system (cf. Lippman and Holman, 1989).

In Fig. 5 it is first seen how the initial perturbation with a wave length of $3200 \text{ m}/3 = 1070 \text{ m}$ emerges. This wave length is similar to the 1100 m found in the linear analysis of Deigaard

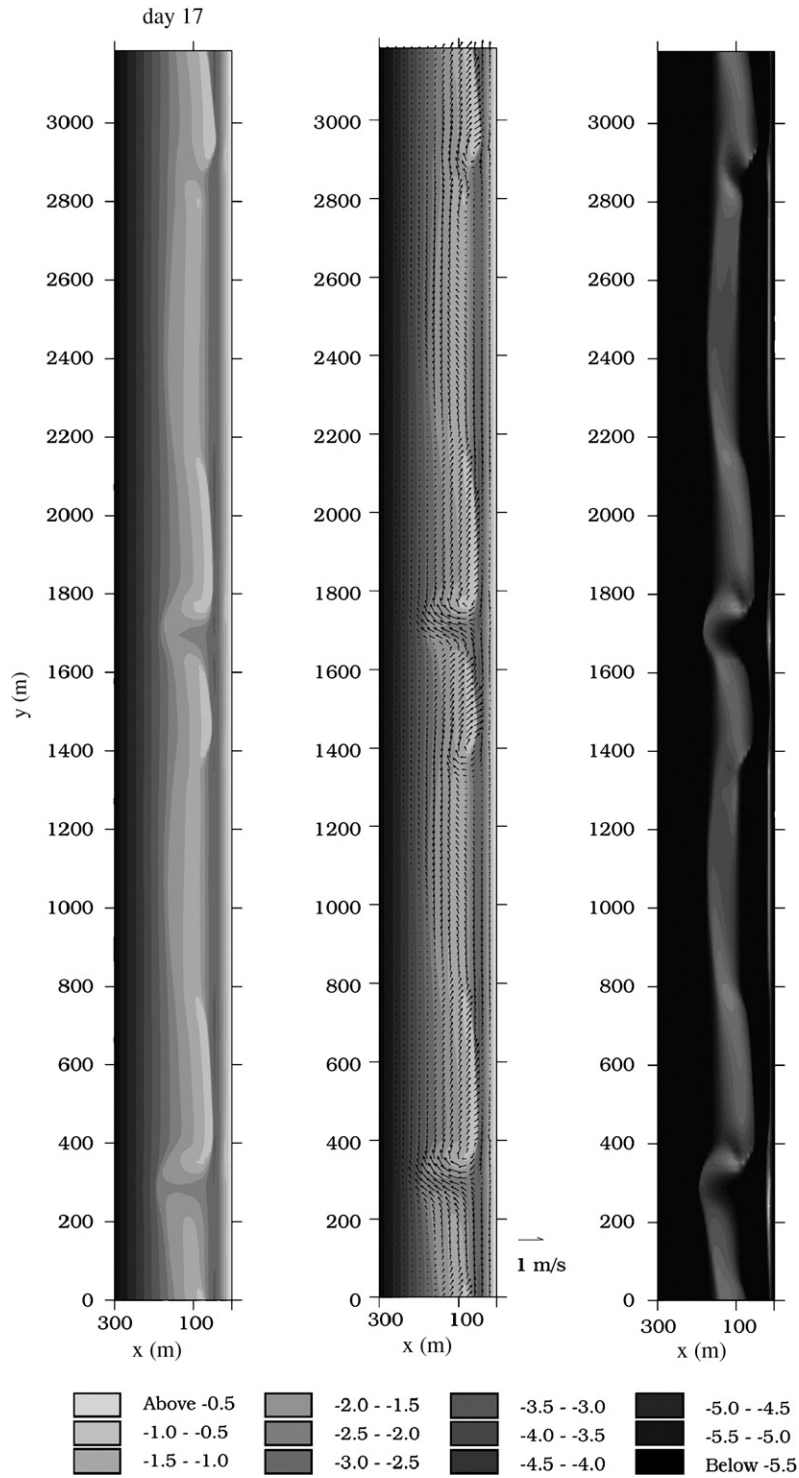


Fig. 6. The final bathymetry after 17 days of simulation with the 2DH model, wave angle: 20°. Left: bathymetry. Centre: flow pattern. Right: distribution of wave energy dissipation.

et al. (1999), the shape of the perturbation in the initial phases is also in agreement with the linear analysis. The morphological development is mainly caused by the cross-shore flow: accretion and onshore movement of the bar crest at locations with onshore flow and erosion at locations with offshore directed flow. The development just after the first phase with

linear conditions is noticeable. It is clear that the effect of accretion at the bar at inflow areas is stronger and more localised than the outflow, and that the development is in the form of growing mounds rather than eroding rip channels. Later rip channels form upstream of each mound. When formed the rip channels get more and more pronounced with a mound being

formed also upstream of the channel. This sequence of mound-channel formation can also be observed in the simplified morphological bar model of Hansen et al. (2004).

Each rip channel generates a strong circulation pattern with an offshore directed flow through the channel and onshore flow over the adjacent bar sections. A tendency can be observed for the formation of more circulation cells with offshore flow upstream of the groups of two mounds and a rip channel (at the locations around y equal to 1200 m and 2400 m in Fig. 6) this may be an indication that the system tends to evolve towards a shorter spacing of the rip channels than given by the wave length of the most unstable linear perturbation. There are only three wave lengths in the periodic model domain, and the restrictions imposed by the length of the domain may be important, and make it impossible to determine the actual wave length that would be selected for an infinitely long coast.

The perturbations migrate in the direction of the mean longshore transport. The time-variation of the migration rate is shown in Fig. 7. The initial migration rate is 40–50 m/day and decreases to 10 m/day as the magnitude of the perturbation increases and more erosion/deposition is required to shift the pattern for example by filling in a rip channel at the up-drift side and eroding at the down-drift side.

The 2DH model includes only the destabilising effects associated with the two-dimensional horizontal circulation pattern and not any stabilising effect which may be due to three-dimensionality. The exact relevance of such models is therefore difficult to judge. It clearly gives non-trivial simulation results on the development after the onset of an instability, for example showing how fast the non-linearities become important and after some days are totally dominant. The applicability of the model to make predictions of the bar geometry is limited, for example to predicting the short term development of a bar with known initial geometry.

Another simulation has been made of the development of a long uniform bar under normal wave incidence (i.e. wave angle zero). Fig. 8 shows the simulated morphology after 30 days. Distinct rip channels have evolved with an average spacing of 600–700 m. There appears to be a tendency for the channels to group together with more extended bar sections between the

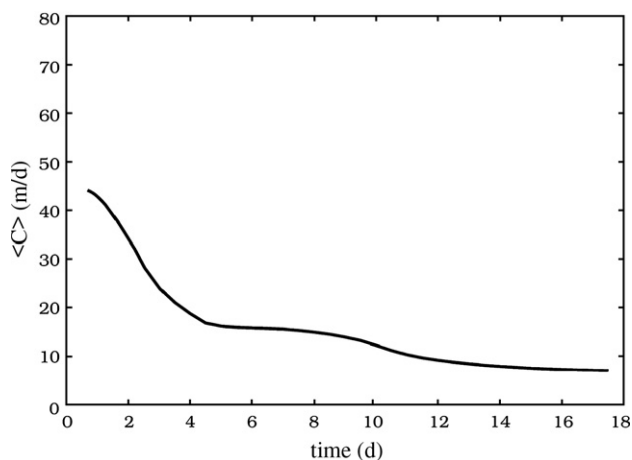


Fig. 7. The time-variation of the migration rate, 2DH simulation, wave angle: 20°.

bars. The grouping gives asymmetry in the strength of the two feeder currents, with the strongest coming from the long bar section, this in turn causes the rip current jets to be oblique. This may reflect an instability of a situation with evenly spaced rip channels. If two rip channels are getting closer to each other by random effects the feeder currents in the trough behind the shorter section of the longshore bar will be slightly weakened. The imbalance in the feeder currents causes an asymmetry which displaces the rip channel towards the weaker current — leading to further reduction of the distance between the two. With five rip channels present in the domain and two long sections of the bar it is unlikely that a tendency for a decrease in the wave length is suppressed by the finite length of the model domain. It is possible that the uneven spacing of the rip channels is the first step in a process leading to the development of a dynamic equilibrium with rip channels decaying or merging and new rip channels emerging (cf. Hansen et al., in 2004). As described, the present model setup does not lead to an equilibrium, because the emergence of very steep bed gradients.

6. One-dimensional profile modelling

The Q3D sediment transport model will give a distinct offshore directed sediment transport in the surf zone, where an undertow is associated with the energy dissipation and the surface rollers of the breaking and broken waves. The offshore transport increases with the distance from the coastline and causes erosion near the shoreline and deposition around the breaker line. This is an important mechanism in the formation of a breaker bar (cf. e.g. Dally and Dean, 1984; Brøker Hedegaard et al., 1991; Roelvink and Brøker, 1993), and in the present model the evolution of the longshore bars is driven by this mechanism.

The Q3D transport model is in principle a local model, where for example the sediment transport is determined from the local forcing. In the surf zone there is a very direct coupling between the local water depth and the forcing of the undertow, because the energy dissipation is depending on the ratio between the water depth and the wave height. The development of the profile resulting from this forcing and the application of a local model give a rapid development of a coastal profile with very steep gradients in the bed surface and in the cross-shore profile. There are a number of physical mechanisms, which are not included in the Q3D model approach. The development of a realistic bar profile in a model requires the representation of processes which redistribute the undertow and the transport relative to the local forcing as illustrated by Brøker Hedegaard et al. (1991) and Fredsøe and Deigaard (1992). Such effects can be due to the gradual development in the breaking process, hysteresis in the conditions for the onset and cessation of wave breaking, the gradual adaptation of the undertow to the shear stress from surface rollers, the inertia in the undertow and lag effects in the development of suspended sediment concentration profiles. In a Q3D model based on depth integrated flow simulations it is not attempted to describe the processes in detail. Instead the combined effect of these processes is schematised by introducing smoothing and lag effects in

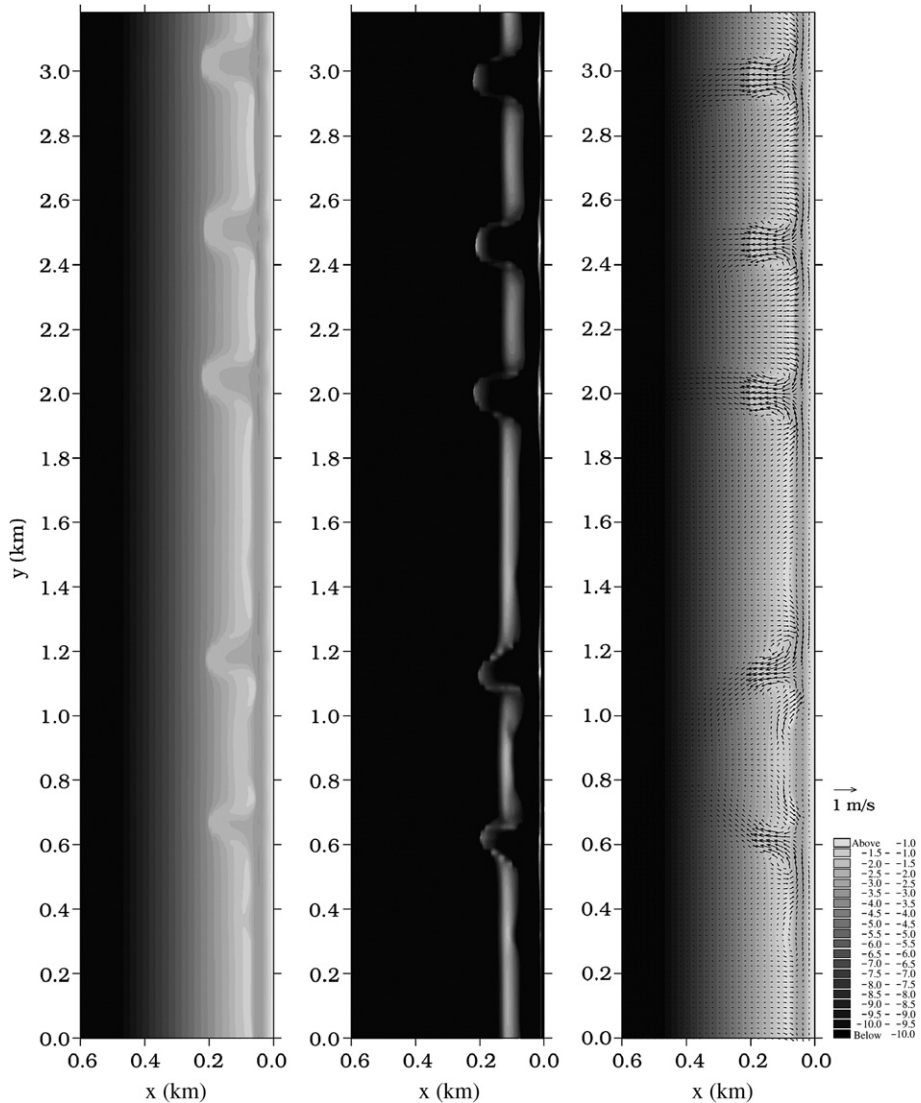


Fig. 8. The simulated morphology after 30 days, 2DH model with normal wave incidence. Left: bathymetry. Centre: distribution of wave energy dissipation. Right: Flow pattern.

description of the sediment transport. It is not expected to be possible to obtain a realistic bar profile by including the undertow in a Q3D model without resorting to a significant smoothing and/or lag effect in the forcing or the transport field, and the authors are not aware of a well documented model, which can simulate the formation and development of a bar profile without including such effects.

Simulations with and without lag are shown in Fig. 9. Fig. 9A shows a simulation applying the local sediment transport only. No roller lag on the forcing has been introduced. It is seen how a front is formed, progressing in the offshore direction. The front is steepening as it develops and no bar is generated in this case.

A lag is introduced in the model by including the effect of a roller lag of ten times the local depth. The result is shown in Fig. 9B. The profile is still forming a very steep front migrating offshore. The effect of the roller lag is the sharp peak formed at the front. The horizontal length scale of the peak is determined

by the lag distance of the roller, i.e. the distance over which the roller grows until it reaches its equilibrium volume.

In a one-dimensional model the smoothing may be represented by modifying the local sediment transport field, q_{so} , according to the diffusive procedure:

$$\frac{\partial}{\partial x} \left(\varepsilon \frac{\partial q_s}{\partial x} \right) = q_s - q_{so} \tag{16}$$

Where ε represents a smoothing coefficient and q_s is the smoothed transport. The profile after a simulation period of 14 days is shown in Fig. 10A with ε equal $100D^2$ corresponding to a smoothing length scale of $10D$. Fig. 10A shows the profile with smoothing but no lag. It should be noted that ε is quantified by the local water depth and therefore varies across the profile and decays towards the coastline. It is seen that the effect of the diffusion is not only to smooth the front but also to make a bar form.

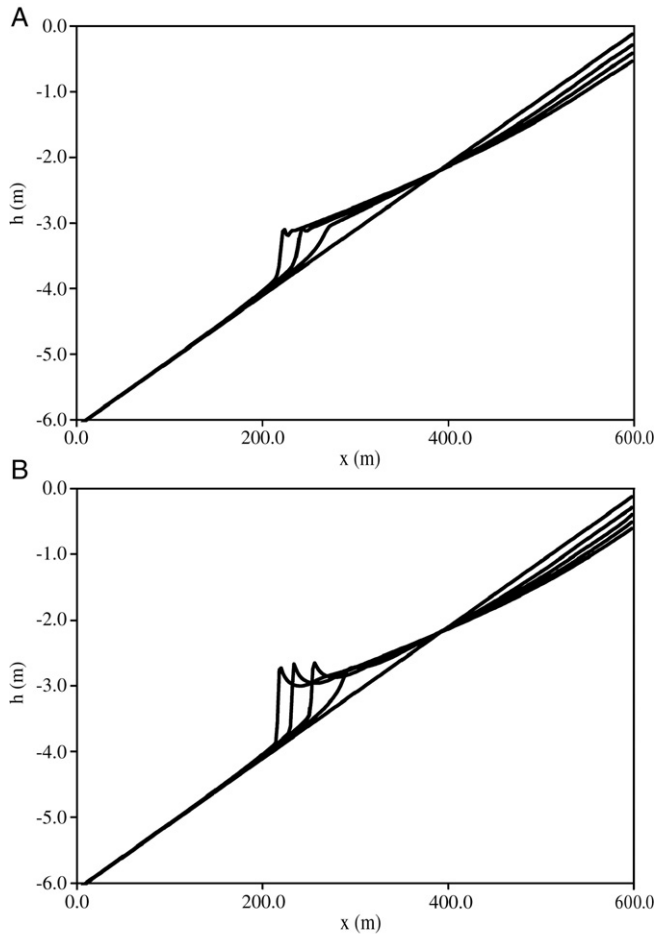


Fig. 9. Profile simulations. A: no lag or smoothing introduced (profiles after 3, 6 and 9 days). B: Roller lag introduced in the wave forcing (profiles after 4, 8, 12 and 14 days), cf. Dally and Brown (1995).

Fig. 10B shows the profile simulated with the combined effect of roller lag and transport diffusion. Again a barred profile has emerged. The effect of the roller lag is to increase the bar crest giving a more pronounced bar and trough profile. There is also a tendency for the formation of an inshore secondary bar being formed by the waves breaking a second time after being reformed, having passed the outer bar. This combination (roller lag length: $10D$ and diffusivity: $100D^2$) was chosen as the basic setting for the model runs with the Q3D model, as the predicted development of the bar profile was considered to be most realistic with both processes included. It should be noted that the primary purpose of this work is to study the model principles and the overall behaviour of the model complex, and not — at this point — to apply the model for actual prototype predictions.

When the procedure is extended to the full Q3D model the redistribution due to the diffusion is made along the wave rays (similar to the introduction of the roller lag).

The angle of wave approach is one of the most important parameters for the coastal morphology. In Fig. 10C the results from running the model with different wave angles in the range from 0° to 40° is shown. The model includes wave refraction and longshore current, but it is still one-dimensional with complete alongshore uniformity. It is seen that a longshore bar

is formed for all the wave angles considered, but the trough is less pronounced for the more oblique wave incidence, and the bar crest has progressed less offshore and has a slightly higher crest elevation.

This is primarily due to the lower shore-normal wave energy flux and the effect of wave refraction, which gives a smaller breaker height and driving force for the undertow for oblique wave incidence. The longshore current increases with the wave

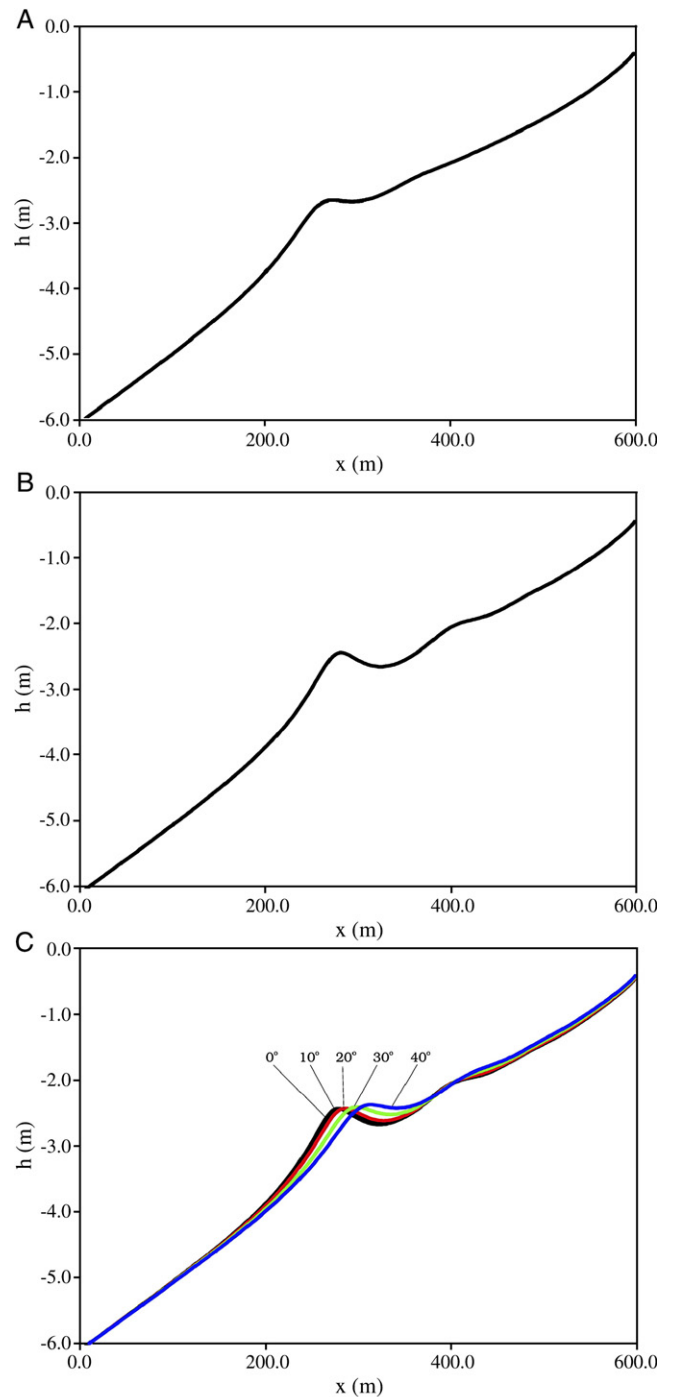


Fig. 10. Profile simulations. A: profile after 14 days, smoothing introduced. B: profile after 14 days, with smoothing and roller lag. C: As B, but for different deep water wave angles.

angle for angles less than approximately 45°. The effect of the longshore current is mainly due to an increase in the eddy viscosity, which is felt as an increased flow resistance and causes a reduction in the strength of the undertow velocity, but at the same time the longshore current causes an increase in the suspended sediment concentration. More details on the effect of the wave direction for the evolution of a longshore bar are given by Elfrink et al. (2000).

7. Q3D area modelling

7.1. Processes for bar formation in the area model

The redistribution of the sediment transport used in the profile model is also introduced in the general Q3D model. The two-dimensional instability mechanism associated with the horizontal circulations is better understood and more robust than the details in the bar-forming mechanism. If the bars were evolving with very steep profiles as in Fig. 9A the hydrodynamic model is likely to blow up and in this way the smoothing can be said to stabilise the simulations. It should be noted that, as described by Eq. (14), the sediment transport rate is composed of a contribution $\vec{q}_{st,c}$ related to the depth integrated flow vector and a contribution $\vec{q}_{st,Q}$ related to the deviation from the depth integrated flow vector, and that the smoothing and lag is only applied to the latter. In this way the effect of the smoothing is only applied to the part of the transport related to the undertow so that its effect is minimized. The profile generating mechanism is therefore consistent with the one-dimensional profile model and the two-dimensional horizontal instability mechanism is consistent with the depth integrated modelling.

7.2. Examples of simulations

Simulations are made for a model domain of 2000 m by 800 m and an initial beach slope of 1:100. The grain size of the bed sediment is $d_{50}=0.15$ mm. Settling velocity of sediment: $w_s=0.013$ m/s. The momentum exchange coefficient is taken to be 0.2 m²/s which is larger than the 0.01 m²/s used for the 2DH model simulations. Both values are rather small and the change is not expected to have drastic consequences for the outcome of the hydrodynamic simulations, but the higher value is considered more realistic. The Q3D simulation starts from a uniform coast which has been through 14 days of profile development as described by the one-dimensional model, cf. Fig. 10. The outer bar is seeded with small random perturbations, as described for the 2DH simulations.

The Q3D simulations are compared qualitatively to the predictions made by the 2DH model, but a direct quantitative comparison is not possible because the bar profile evolves continuously during the Q3D simulation, while the 2DH model simulates the development of a prescribed bar profile which is given at the start of the simulation. The width of the domain for the 2DH simulations is similar to the domain used for the stability analysis of Deigaard et al. (1999), while the width of the Q3D domain is larger because the first bar is migrating

offshore during the entire simulation period. The duration of the Q3D simulation is longer, and to limit the computational effort the domain is made shorter than in the 2DH simulations.

7.2.1. Oblique wave incidence

The basic example with oblique wave incidence has the deep water wave parameters: $H_{rms}=1.0$ m, $T_p=7.5$ s and $\theta_0=15$. The temporal development is illustrated in Fig. 11. In Fig. 12 the morphology for the last time step of the simulation (after 40 days of Q3D following the 14 days of profile simulation) is shown with the flow pattern and distribution of wave energy dissipation.

In the later part of the simulation the model develops several bars — ending with a series of 5 bars. The multi-bar system is generated because the wave breaking ceases in the trough inshore of a bar. The next breaker line then determines the position and development of the next bar. Systems of several longshore bars are known from field conditions, for example at the Dutch and the Danish North Sea coast and at coasts of the inner Danish Waters where two or three bars are frequently observed. Large scale flume experiments also show several (up

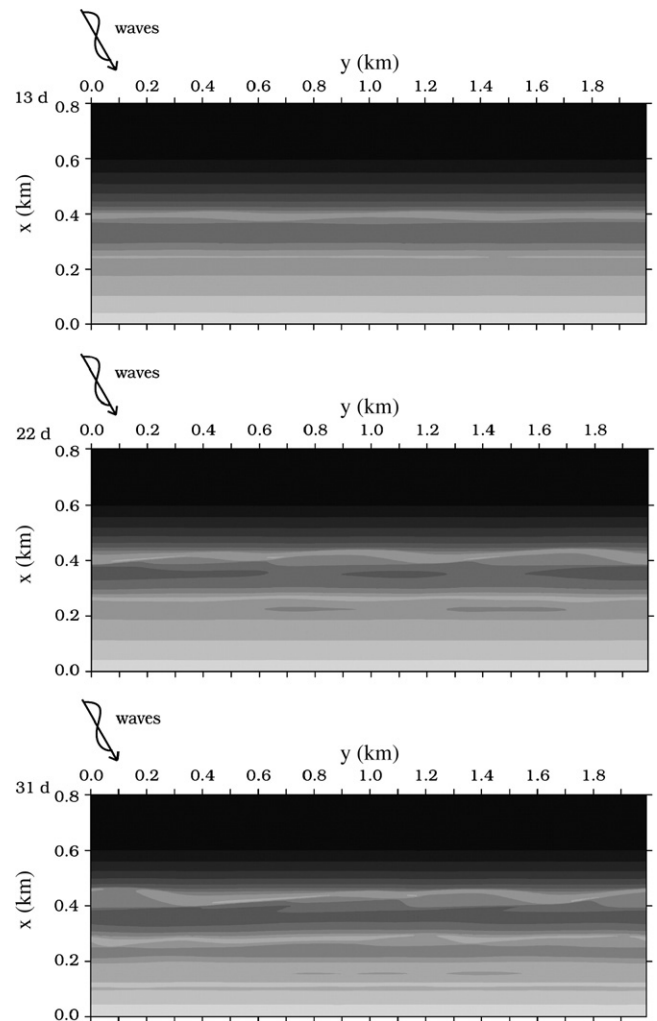


Fig. 11. Temporal development of the coast in the Q3D model, Bathymetry after 13, 22 and 31 days. The Q3D model has been started on a uniform bathymetry obtained after 14 days simulation with the profile model only. Wave angle: 15°.

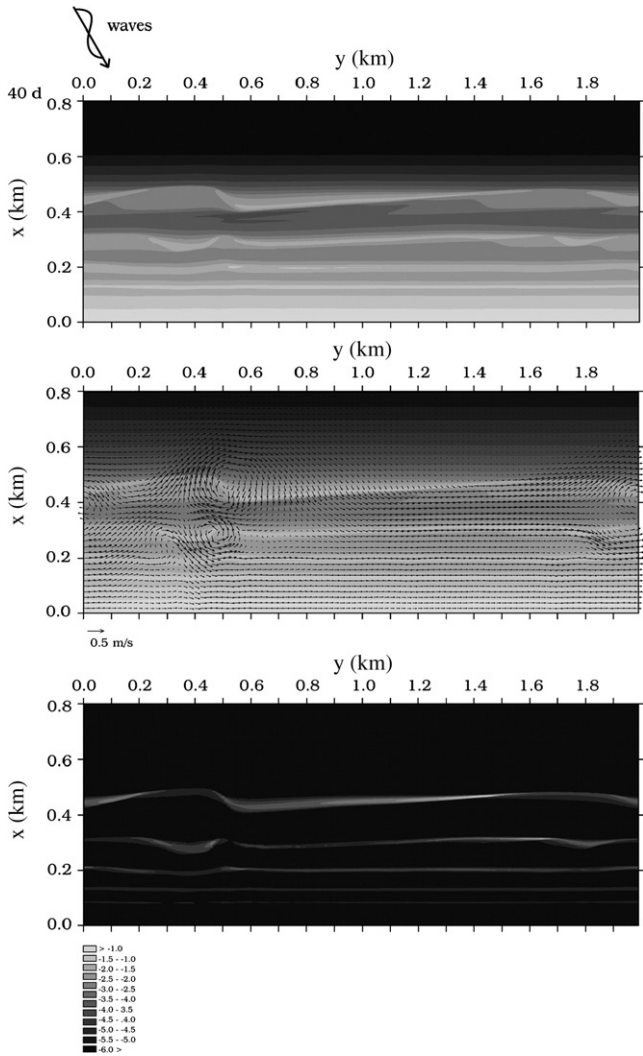


Fig. 12. The final bathymetry after 40 days of Q3D simulations. Top: bathymetry, Middle: flow pattern, Bottom: distribution of wave energy dissipation.

to five) bars as seen in the experiments of Saville (1957) and Dette and Uliczka (1986). While a theoretical model may predict a very large number of bars formed by the mechanism described above, effects in nature such as the presence of low frequency waves may suppress the formation of very small and short bars near the shoreline because near the shore line the low frequency variation in the water level becomes large compared to the height of the short breaking waves.

The 2DH part of the model causes an instability in the outer bar as it evolves and migrates offshore. Large scale skew features are formed as weak undulations. As they grow in amplitude they attain an along-shore wave length of about 600–700 m. The features migrate along the shore at a rate of 20–30 m/day. Water is pushed onshore over the bar crest by the gradient in the shore-normal radiation stress, building up a feeder current in the trough. As the feeder current is built up, the bar crest position changes along the coast, forming a long oblique bar shape. The oblique bar terminates at a depression or ‘rip channel’ where the flow is directed offshore, and the flow in

the trough down-drift of this rip is reversed as also seen in the pure 2DH simulations. The longshore velocity is generally stronger in the trough inshore of the outer bar than on the bar itself, which is in contrast to the conditions on a uniform barred coast. Erosion occurs in the trough (local deepening of the trough) due to the alongshore acceleration of the feeder current.

The inner bars do not spontaneously generate alongshore variability as the outer bar does. The variation along the inner bar is a reflection of the variation in the crest elevation and circulation currents generated over the outer bar. It may be noted how the crest position and circulation current in the second bar are opposite those of the outer. The depression of the bar crest at the outflow area on the outer bar allows more wave energy to pass. The higher waves in turn causes onshore flow and displacement in the onshore direction of the crest of the second bar.

Fig. 13 shows a three-dimensional view of the bathymetry taken at day 22 (following the first 14 days of profile simulation) in the simulation.

7.2.2. Normal wave incidence

The morphological development is completely different for normal wave incidence. Fig. 14 shows the flow field and distribution of wave energy dissipation at the end of the simulation after 12 days of Q3D following the 14 days of profile simulation. The alongshore length scale is much smaller than for oblique wave incidence, and the outer bar shows a distinct pattern resembling crescentic bars. Like the case with oblique incidence, the length scale of the variations along the outer bar is also imprinted on the inner bars. The onshore directed flow

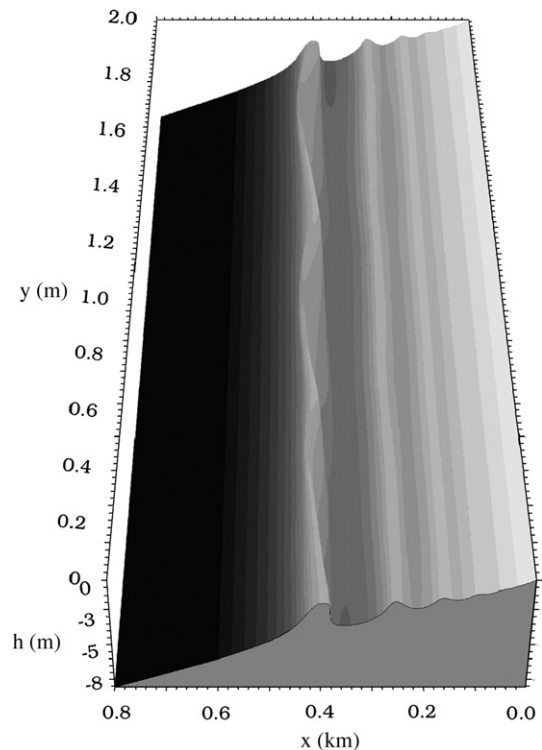


Fig. 13. Three-dimensional illustration of the bathymetry after 22 days of Q3D simulation. Wave angle: 15°.

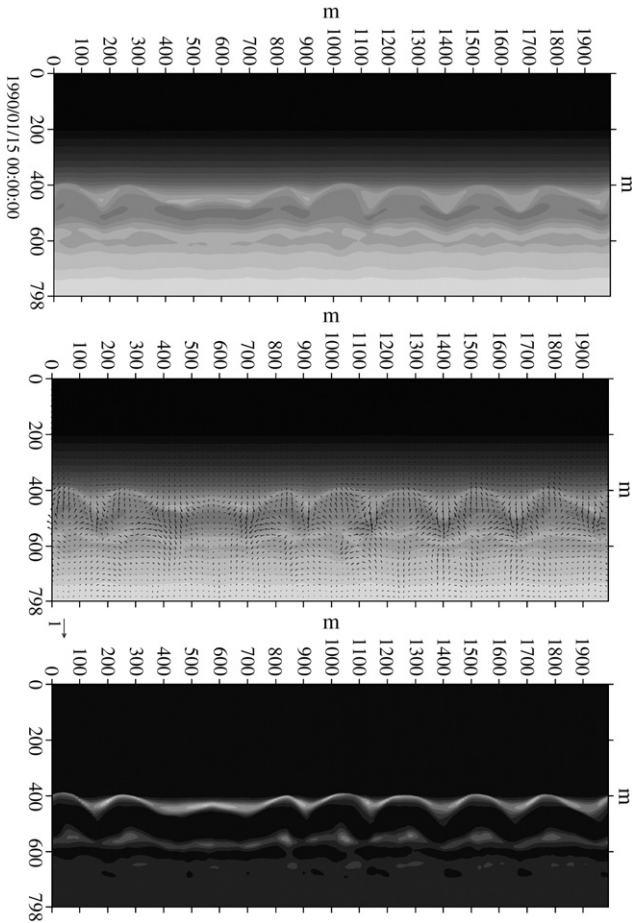


Fig. 14. The bathymetry, flow field and distribution of wave energy dissipation at the end of the simulation with normal wave incidence, after 12 days of Q3D following 14 days of profile simulation.

over the shallow parts of the outer bar is stronger and more concentrated than the offshore directed. It is seen how the sand has been accumulated in lobe-shaped mounds pointing onshore at the locations of onshore flow.

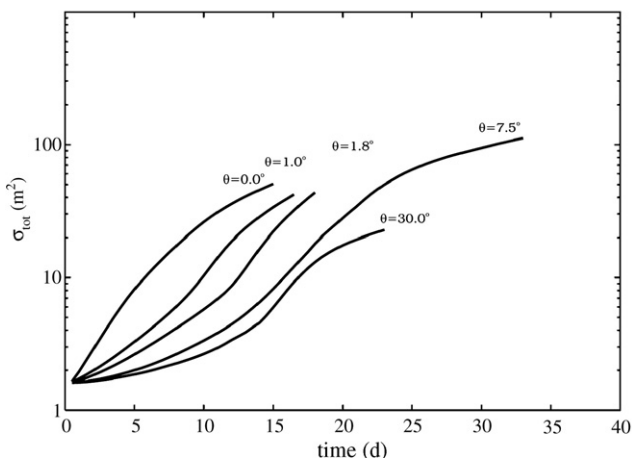


Fig. 15. The temporal development of the total alongshore variance for different wave angles.

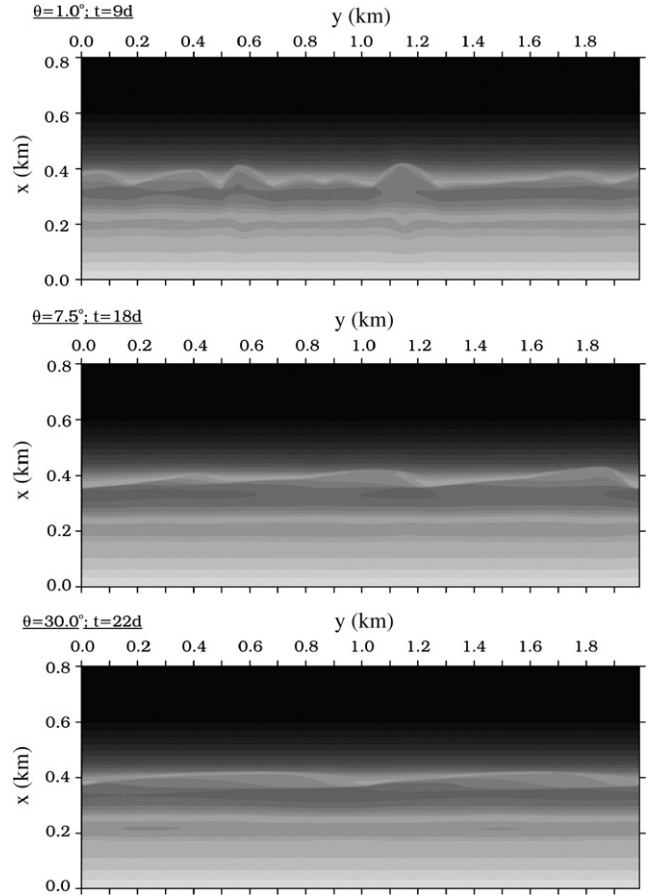


Fig. 16. Examples of bathymetries simulated by the Q3D model for different wave angles. The three bathymetries have the same value of the alongshore variance, $\sigma_{tot} = 20 \text{ m}^2$, and are consequently taken at different times in the simulation: after 9, 18 and 22 days of Q3D simulation.

When comparing the 2DH and Q3D simulations it is clear that the inclusion of the undertow as a bar-forming mechanism has a significant effect on the bar morphology. Both for oblique and normal waves the rip channels are much less pronounced and less localised in the Q3D simulations. The difference is most striking for normal wave incidence, where all of the outer bar is undulating while in the 2DH model the bar consists of almost straight sections separated by rip channels.

7.3. The sensitivity to variation in the wave direction

Simulations have been performed for a range of wave directions to investigate the significance of the incident wave direction, as was also done by Calvete et al. (2005). In Fig. 15 the temporal development of the alongshore variance (defined in Eq. (15)) is shown for different wave angles. It is seen that the growth rate decreases with increasing angle. Small angles correspond to a more unstable morphology both in the initial and the later parts of the evolution. The sensitivity at small angles is remarkable, there are clear differences between the development at 0° , 1° and 1.8° situations, which in field conditions all may be characterised as normal wave incidence.

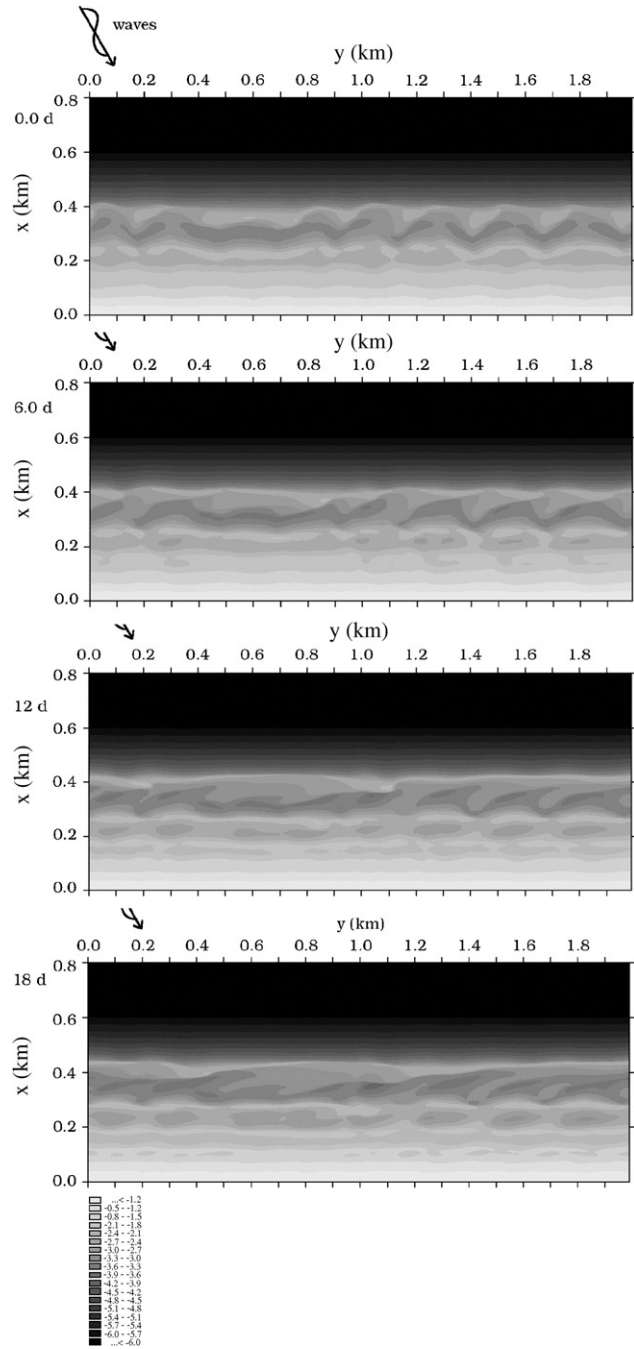


Fig. 17. Development of a bathymetry after a change in wave direction from normal incidence to a wave angle of 30°.

The development for 0° wave angle is qualitatively different from the rest. For all the finite angles the curves are S-shaped with a slow initial growth followed by a significant increase in the growth rate, which eventually tends to decrease again towards the end of the simulation (the plot is semi-logarithmic, so the growth rates in question are exponential). The duration of the different phases is dependent on the wave angle. The more pronounced the trough inshore of the first bar the stronger the instability mechanism, which explains why the growth rate increases after the initial relatively stable phase. As seen from Fig. 10C the trough is smaller for the larger angles with the

longest duration of the initial phase. For a 0° wave angle the perturbations grow fast from the start of the simulation without the initial phase of slow growth.

Fig. 16 shows three examples of bathymetries for different wave angles. The bathymetries shown have the same value of the alongshore variance, $\sigma_{tot}=20 \text{ m}^2$, and are consequently taken at different times in the simulation. It may be noted that the configuration for $\theta=1^\circ$ is qualitatively similar to the bar formed by normally incident waves, even though the initial temporal development is slower as described above.

An impression of the model results for a variable wave condition can be obtained from Fig. 17, which shows a situation with transition from normal to oblique wave incidence. The start of the simulation is the final bathymetry after the simulation with normal wave incidence. From that stage the wave direction has been changed to 30° and the simulation continued for 18 days. The oblique waves modify the outer bar towards the more alongshore uniform configuration found for simulations with oblique waves only. First the features are becoming skew and as a slower process the wave length along the bar increases from 200–250 m to the order 1 km found for the oblique waves. This evolution is partly due to the bar generating mechanisms: when the wave angle is increased the circulation currents over the bar is reduced, and the Q3D part of the transport (undertow) becomes more important for the cross-shore exchange of sediment.

The morphology in the trough and bars inshore of the first bar maintain smaller features from the initial conditions with normal wave incidence, although oblique secondary bars also appear due to the longshore current formed in the trough.

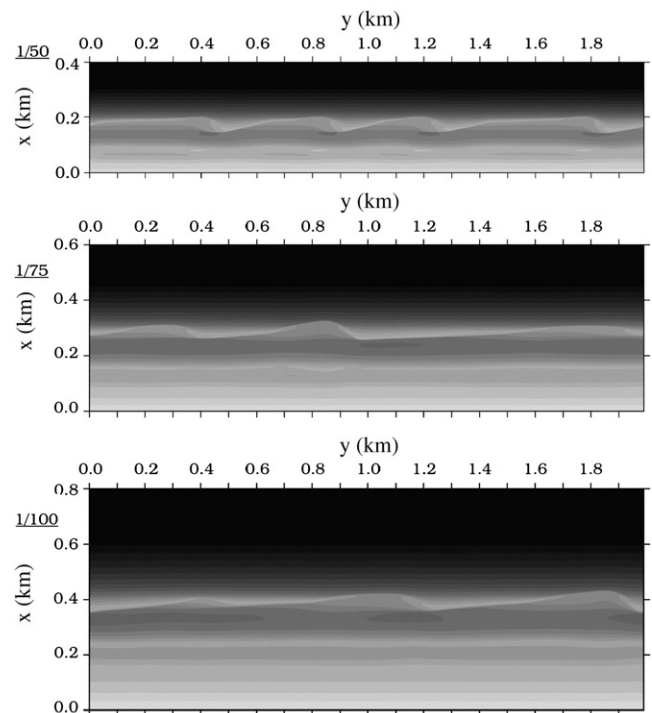


Fig. 18. The morphology for different beach slopes, Q3D model. Alongshore variance, $\sigma_{tot}=20 \text{ m}^2$.

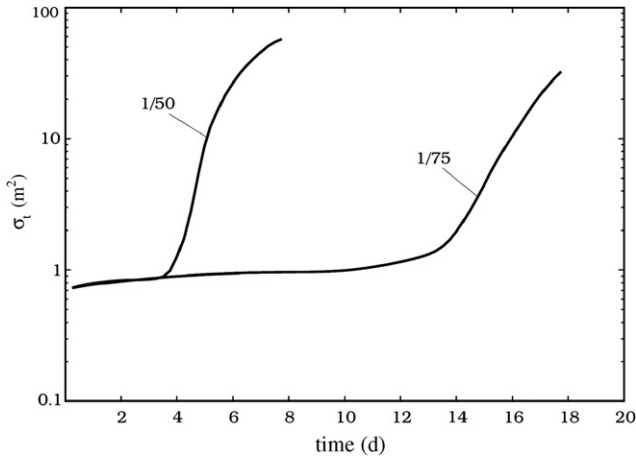


Fig. 19. The temporal evolution of the alongshore variance for two beach slopes: 1/50 and 1/75.

7.4. Sensitivity to the beach slope

The significance of the initial (or ‘gross’) beach slope was investigated by simulations for beaches steeper than the 1:100 used for the basic simulations.

For oblique waves a wave angle of 7.5° was applied. Fig. 18 shows three bathymetries with identical alongshore variability ($\sigma_{\text{tot}} = 20 \text{ m}^2$) and slopes of 1:50, 1:75 and 1:100. The alongshore wave length is clearly smallest for the steepest beach which is to be expected as the distance from the shoreline and the cross-sectional area of the trough is smaller for the steeper beach. In Fig. 19 the development in the alongshore variance is illustrated for the two steeper beach slopes. The time needed for the onset of a rapid development in the bathymetry is seen to be smaller for the larger slope. The faster development of the instabilities for a steeper beach is to be expected, because the cross-shore gradients in all processes are inversely scaled with the beach slope.

A simulation has been made with normal wave incidence and a beach slope of 1:50. After 4.5 days alongshore uniform profile simulation and 1.5 days of Q3D simulation the pattern is qualitatively similar to the 1:100 beach slope simulation, but with a reduced alongshore wave length (of about 150 m), as was also found for the oblique wave incidence.

7.5. Sensitivity to the wave height

Simulations with a reduced wave height (deep water wave height $H_{\text{rms}} = 0.7 \text{ m}$, wave angle: 7.5°) gave a configuration of the outer bar similar to the basic example, but with a reduced alongshore wave length of 400 m (the dimensions of the model domain was unchanged: 800 m by 1800 m), due to the reduced length scale of the outer bar (water depth over the crest, distance from the shoreline and cross-sectional area of the trough) and the reduced longshore current velocity.

8. Conclusions and discussion

The study has been made to investigate if inclusion of bar-forming mechanisms changes the results of morphological

models, compared to depth integrated models where the sediment transport is taken to follow the direction of the depth integrated flow velocity. Further it is of interest if the Q3D model with bar formation has improved characteristics compared to the 2DH model, for example if the combination of undertow and horizontal circulations makes the simulations reach a dynamic equilibrium where the statistical properties of the bar morphology is constant even though the bar configuration is changing. The new aspects of the Q3D model study is that situations with oblique wave incidence and longshore currents are considered, and that the longshore bar system has been formed from an initially plane, constant slope, beach. The purpose has thus been to analyse the significance of including of specific elements into a model and to see if it leads to qualitatively different predictions. It has not been the purpose to make simulations of specific field conditions to try to validate the model system. It is not expected that models at the present stage of development are sufficiently advanced to allow for a detailed quantitative verification.

One of the difficulties in the present study is the comparison between the 2DH model and the Q3D model. Both model produce simulations where the morphology of near-shore bars evolve from a bathymetry with alongshore uniform profiles. The evolution progresses on both cases with increasing variation in the alongshore direction and no (dynamic) equilibrium is reached for any of the models. It is not possible to make a direct comparison between the two models, because in the Q3D model the bar geometry (e.g. the mean depth over the bar crest and the position of the bar) is changing continuously. It is therefore not possible to select a single profile for the 2DH model for making the comparison.

8.1. Specific conclusions

A Q3D morphological area model has been developed, which includes horizontal wave-driven circulation currents as well as mechanisms forming a longshore bar through the effect of the undertow current in the surf zone. The formation of a longshore bar with a distinct trough inshore of it requires the inclusion of lag and smoothing of the Q3D sediment transport field.

The model predicts a dynamic evolution of a barred coast with a coastal profile developing simultaneously with the formation of irregularities in the longshore bar. Comparison between simulations made by the Q3D model and results from a depth integrated 2DH model without bar-forming mechanisms demonstrates some noticeable differences:

- For oblique wave incidence the morphology is much more uniform when the Q3D effects are included, the rip channels are wider and less distinct.
- For normal wave incidence the Q3D model gives a rhythmic crescentic longshore bar, while the 2DH model produces a number of pronounced rip channels separating a series of almost straight sections of the longshore bar.

The differences are much more pronounced than can be explained by the relatively small difference in the turbulent exchange factor in the simulations, and the lag and smoothing in the Q3D model are only applied to the sediment transport related

to the Q3D effects in the form of the undertow. Physically, the more uniform bathymetry for the Q3D model may be related to the undertow counteracting the horizontal circulation currents. As described in the introduction a bar section with increased crest elevation will cause an increase in the energy dissipation due to the wave breaking, which in the 2DH model gives an onshore directed flow and sedimentation. The undertow is also related to the wave energy dissipation, and an increased dissipation gives an increased undertow and a tendency for erosion.

Both model types predict a shorter alongshore wave length of the bar morphology for normal wave incidence than for oblique wave incidence, which is in agreement with the stability analysis of Deigaard et al. (1999). The temporal development of the bar irregularities is slower for oblique wave angles.

A simulation with the Q3D model illustrates the transition from conditions of normal wave incidence to oblique waves. The crescentic bar features become skew, and gradually the alongshore wave length of the variation of the longshore bar increases, while relict forms with the initial shorter wave length continue to exist in the bar trough.

Simulations with different initial steepness of the coastal profile shows the alongshore wave length to decrease and the temporal development to be faster for a steeper beach. This reflects the stronger energy dissipation and the smaller volumes involved in the profile development for a steeper profile for a given incident wave condition.

The present work has concentrated on the effects of including mechanisms for bar formation in a morphological area model for coasts with longshore bars. There are a number of other processes, which has not been considered in this context, such as diffraction and current refraction of the incoming waves, grouping of incident waves, low frequency waves, shear waves in the longshore current. These could be of importance for modelling the near-shore morphology and may be of significance for the quality of future morphological simulation models. A significant uncertainty of the present model is the representation of the lag and smoothing effects in the Q3D model and the underlying physical mechanisms. It is possible that these may to some degree be related to some of the processes mentioned above, but are probably mainly due to the assumption of locality in Q3D models. To overcome the lag and smoothing the inertia and temporal and spatial development in the sediment concentration field must be described by the model, which probably will require a much more complex model with a fully three-dimensional hydrodynamic and sediment transport model.

Acknowledgement

The present work has been supported by the Danish Research Council for Technology and Production Sciences (Forskningsrådet for Teknologi og Produktion) under the frame programme 'Exploitation and Protection of Coastal Zones' (EPCOAST).

References

Battjes, J.A., Janssen, J., 1978. Energy loss and set-up due to breaking in random waves. Proc. 16th Int. Conf. on Coastal Eng. ASCE, Hamburg, pp. 569–587.

- Black, K.P., Gorman, R.M., Bryan, K.R., 2002. Bars formed by horizontal diffusion of suspended sediment. Coastal Engineering 47, 53–75.
- Boczar-Karakiewicz, B., Bona, J.L., Cohen, D.L., 1987. Interaction of shallow water waves and bottom topography. Dynamical Problems in Continuum Physics, vol. 4. Springer Verlag, Heidelberg, pp. 131–176.
- Brøker Hedegaard, I., Deigaard, R., Fredsøe, J., 1991. Onshore/offshore sediment transport and morphological modelling of coastal profile. Proc. Coastal Sediments '91. ASCE, Seattle, pp. 643–657.
- Caballeria, M., Coco, G., Falques, A., Huntley, D.A., 2002. Self-organization mechanisms for the formation of nearshore crescentic and transverse sand bars. Journal of Fluid Mechanics 465, 379–410.
- Calvete, D., Dodd, N., Falques, A., van Leuwen, S.M., 2005. Morphological development of rip channel systems: normal and near-normal wave incidence. Journal of Geophysical Research 110, C10006. doi:10.1029/2004JC002803.
- Christensen, E.D., Deigaard, R., Fredsøe, J., 1994. Sea bed stability of a long straight coast. Proc. 24th Int. Conf. on Coastal Eng. ASCE, Kobe, pp. 1865–1879.
- Dally, W.R., Brown, C., 1995. A modeling investigation of the breaking wave roller with application to cross-shore currents. Journal of Geophysical Research 100 (C12), 24,873–24,883.
- Dally, W.R., Dean, R.G., 1984. Suspended sediment transport and beach evolution. Journal of Waterway, Harbors, Coastal, and Ocean Engineering Division (ASCE) 110 (WW1), 15–33.
- Damgaard, J., Dodd, N., Hall, L., Chesher, T., 2002. Morphodynamic modelling of rip channel growth. Coastal Engineering 45 (3–4), 199–221.
- Dean, R.G., Srinivas, R., Parchure, T.M., 1992. Longshore bar generating mechanisms. Proc. 23rd Int. Conf. On Coastal Eng. ASCE, Venice, pp. 2001–2014.
- Deigaard, R., 1989. Mathematical modelling of waves in the surf zone. Progress Report No. 69, Inst. of Hydrodynamics and Hydraulic Engineering (ISVA). Technical University of Denmark, pp. 47–60.
- Deigaard, R., 1993. A note on the three-dimensional shear stress distribution in a surf zone. Coastal Engineering 20, 157–171.
- Deigaard, R., Fredsøe, J., 1989. Shear stress distribution in dissipative water waves. Coastal Engineering 13, 357–378.
- Deigaard, R., Fredsøe, J., Brøker Hedegaard, I., 1986. Suspended sediment in the surf zone. Journal of Waterway, Port, Coastal, and Ocean Engineering (ASCE) 112 (1), 115–128.
- Deigaard, R., Drønen, N., Fredsøe, J., Jensen, J.H., Jørgensen, M., 1999. A morphological stability analysis for a long straight barred coast. Coastal Engineering 36 (3), 171–195.
- Detle, H., Uliczka, K., 1986. Seegangserzeugte Wechselwirkung zwischen Vorland und Vorstrand sowie Küstenschutzbauwerk. Technischer Bericht N. 3 – SBF 205/TP A6. Universität Hannover.
- DeVriend, H.J., Stive, M.J.F., 1987. Quasi-3D modeling of nearshore currents. Coastal Engineering 11 (5–6), 565–601.
- DeVriend, H.J., Zyserman, J., Nicholson, J., Roelvink, J.A., Pechon, P., Southgate, H.N., 1993. Medium-term 2DH coastal area modelling. Coastal Engineering 21 (1–3), 193–224.
- Dingemans, M., Radder, A., DeVriend, H.J., 1987. Computation of driving forces of wave-induced currents. Coastal Engineering 11 (5–6), 539–563.
- Drønen, N., Deigaard, R., 2000. Three dimensional near-shore bar morphology. Proc. 27th Int. Conf. on Coastal Eng. ASCE, Sydney, pp. 3205–3217.
- Dyhr-Nielsen, M., Sørensen, T., 1970. Sand transport phenomena on coasts with bars. Proc. 12th Int. Conf. On Coastal Eng. ASCE, Washington D.C., pp. 855–866.
- Elfrink, B., Brøker, I., Deigaard, R., 2000. Beach profile evolution due to oblique wave attack. Proc. 27th Int. Conf. On Coastal Eng. ASCE, Sydney, pp. 3021–3034.
- Engelund, F., Fredsøe, J., 1976. A sediment transport model from straight alluvial channels. Nordic Hydrology 7, 293–306.
- Falques, A., Montoto, A., Iranzo, V., 1996. Bed-flow instability of the longshore current. Continental Shelf Research 16 (15), 1927–1964.
- Fredsøe, J., 1984. Turbulent boundary layers in wave-current motion. Journal of Hydrologic Engineering (ASCE) 110 (HY8), 1103–1120.
- Fredsøe, J., Deigaard, R., 1992. Mechanics of coastal sediment transport. Advanced Series on Ocean Engineering. World Scientific, Singapore. 369 pp.

- Fredsøe, J., Andersen, O.H., Silberg, S., 1985. Distribution of suspended sediment under large waves. *Journal of Waterway, Port, Coastal, and Ocean Engineering* (ASCE) 111 (6), 1041–1069.
- Hairer, E., Wanner, G., 1996. *Solving ordinary differential equations, 2, Stiff and Differential Algebraic Problems*. 2nd ed. Springer Verlag.
- Hansen, H.F., Deigaard, R., Drønen, N., 2004. A numerical hybrid model for the morphology of a barred coast with a river mouth. *Proc. 29th Int. Conf. on Coastal Eng. (ASCE)*, Lisboa, pp. 2607–2619.
- Hino, M., 1974. Theory on formation of rip-current and cuspidal coast. *Proc. 14th Int. Conf. on Coastal Eng. ASCE*, Copenhagen, pp. 901–919.
- Holthuijsen, L.H., Booij, N., Herbers, T.H.C., 1989. A prediction model for stationary, short-crested waves in shallow-water with ambient currents. *Coastal Engineering* 13 (1), 23–54.
- Lippman, T., Holman, R., 1989. Quantification of sand bar morphology: a video technique based on wave dissipation. *Journal of Geophysical Research* 94 (C1), 995–1011.
- Lippman, T., Holman, R., 1990. The spatial and temporal variability of sand bar morphology. *Journal of Geophysical Research* 95 (C7), 11,575–11,590.
- Miller, R.L., 1976. Role of vortices in surf zone prediction: sedimentation and wave forces. *Beach and Nearshore Sedimentation*. SEPM Spec. Publication, vol. 23, pp. 92–114.
- Nicholson, J., Brøker, I., Roelvink, J., Price, D., Tanguy, J., Moreno, L., 1997. Intercomparison of coastal area morphodynamic models. *Coastal Engineering* 31 (1–4), 97–123.
- Okayasu, A., Shibayama, T., Horikawa, K., 1988. Vertical variation of undertow in the surf zone. *Proc. 21st Int. Conf. on Coastal Eng. ASCE*, Malaga, pp. 478–491.
- Plant, N., Holman, R., Freilich, M., Birkemeier, W., 1999. A simple model for interannual sandbar behavior. *Journal of Geophysical Research* 104 (C7), 15,755–15,776.
- Rakha, K.A., Deigaard, R., Brøker, I., 1997. A phase resolving cross shore sediment transport model for beach profile evolution. *Coastal Engineering* 31, 231–261.
- Reniers, A.J.H.M., Roelvink, J.A., Thornton, E.B., 2004. Morphodynamic modeling of an embayed beach under wave group forcing. *Journal of Geophysical Research* 109 (C1) (Art. No. C01030).
- Roelvink, J.A., Brøker, I., 1993. Cross-shore profile models. *Coastal Engineering* 21, 163–191.
- Ruessink, B.G., Terwindt, J.H.J., 2000. The behaviour of nearshore bars on the time scale of years: a conceptual model. *Marine Geology* 163 (1–4), 289–302.
- Ruessink, B.G., van Enckevort, I.M.J., Kingston, K.S., Davidson, M.A., 2000. Analysis of observed two- and three-dimensional nearshore bar behaviour. *Marine Geology* 169, 161–183.
- Saville, T., 1957. Scale effects in two-dimensional beach studies. *Trans. 7th Meeting, IAHR, Lisbon*, vol. 1, p. A3.
- Svendsen, I.A., 1984. Mass flux and undertow in the surf zone. *Coastal Engineering* 8, 347–366.
- Svendsen, I.A., Lorenz, R.S., 1989. Velocities in combined undertow and longshore currents. *Coastal Engineering* 13 (1), 55–79.
- Tjerry, S., 1995. Morphological calculation of dunes in alluvial rivers. PhD thesis, Institute of Hydrodynamics and Water Resources (ISVA), Technical University of Denmark.
- Tjerry, S., Fredsøe, J., 2005. Calculation of dune morphology. *Journal of Geophysical Research* 110, F04013. doi:10.1029/2004JF000171.
- van Enckevort, I.M.J., Ruessink, B.G., 2003. Video observations of nearshore bar behaviour. Part 2: alongshore non-uniform variability. *Continental Shelf Research* 23 (5), 513–532.
- van Enckevort, I.M.J., Ruessink, B.G., Coco, G., Suzuki, K., Turner, I.L., Plant, N.G., Holman, R.A., 2003. Observations of nearshore crescentic sandbars. *Journal of Geophysical Research* 109, C06028.
- Yu, J., Mei, C.C., 2000. Formation of sand bars under standing waves. *Journal of Fluid Mechanics* 416, 315–348.